EUROPEAN ORGANIZATION FOR NUCLEAR RESEARCH

CERN/EP 80-142
8 August 1980

FAST-BEAM LASER SPECTROSCOPY OF NEUTRON-RICH BARIUM ISOTOPES

R. Neugart

CERN, Geneva, Switzerland

F. Buchinger*, W. Klempt, A.C. Mueller*, E.W. Otten

Institut für Physik, Universität Mainz, Mainz, Fed. Rep. of Germany

C. Ekström*

Dept. of Physics, Chalmers University of Technology, Gothenburg, Sweden

J. Heinemeier

Institute of Physics, University of Aarhus, Aarhus, Denmark

and

The ISOLDE Collaboration

CERN, Geneva, Switzerland

Isotope shifts and hyperfine structure of the Ba I resonance line $6s^2\ {}^1S_0$ - $6s6p\ {}^1P_1$ ($\lambda = 553.6$ nm) have been measured for $^{139-144}$Ba and ^{146}Ba, using on-line collinear laser spectroscopy. The differences of mean-square nuclear charge radii, as well as the spins and moments of the odd-A isotopes are derived from the results.

INTRODUCTION

Collinear laser spectroscopy [1] has proven to be an ideal tool for studies of isotope shifts (IS) and hyperfine structure (hfs) of radioactive atoms in fast beams [2]. Recently, such an apparatus has been connected to the on-line mass separator ISOLDE-II at CERN. The aim of this experiment is to extend the present knowledge about fundamental nuclear properties such as spins, magnetic moments, electric quadrupole moments and mean-square charge radii into regions far from stability.

Here we present the first results, obtained in a sequence of neutron-rich barium isotopes. Further work at the very neutron-deficient side of this isotopic chain is presently under way.

EXPERIMENTAL PROCEDURE

At ISOLDE the heavy barium isotopes are produced by proton-induced fission in a 10 g/cm^2 high-temperature target[3], irradiated with the 600 MeV beam from the CERN synchro-cyclotron. Reaction products, diffusing out of the target, are ionized on a tungsten surface heated at 2300 °C and accelerated to 60 keV. After electromagnetic mass separation the radioactive barium beams are available with intensities between 10^8 and 10^5 atoms/s, decreasing from ^{139}Ba to ^{146}Ba.

* Present address: EP Division, CERN, CH-1211 Geneva 23, Switzerland

The collinear superposition of this beam with a laser beam allows to exploit the compression of the velocity distribution occurring by acceleration [4]. Since the energy spread of the ions

$$\delta E = \delta (m v^2 / 2) = m v \delta v$$

remains constant, the velocity spread δv along the beam is narrowed in the same measure as the velocity $v = (2 eU / m)^{1/2}$ is increased. Hence, the absorption Doppler width

$$\delta \nu = \nu_0 \delta v / c = \nu_0 \delta E / (2 e U m c^2)^{1/2}$$

can be matched to the natural linewidth of optical transitions. The high resolution and excitation efficiency thus achieved are ideally suited to spectroscopy on the weak beams of radioactive isotopes.

Atomic spectra are made accessible by neutalizing the ion beams in a sodium-vapour cell. Since the cross section for the nearly resonant charge transfer

$$\underline{Ba^+} + Na \longrightarrow \underline{Ba} + Na^+ + 0.07\ eV$$

is substantially higher than the one for kinetic collisions, the phase space distribution of the beam remains nearly unchanged.

We have chosen the atomic ground-state transition $6s^2\ ^1S_0 - 6s6p\ ^1P_1$ (λ=553.6 nm) for which accurate measurements of the IS and hfs in the stable and some neutron-deficient barium isotopes have been performed [5]. This transition is excited by the beam of a frequency-stabilized dye laser, operated with rhodamine 110. The large Doppler shift in the 60 kV beam (about 500 GHz, corresponding to 0.5 nm) is used to tune the resonances of different isotopes to the fixed laser frequency. For this purpose the charge-exchange cell is designed as an integral part of a retardation system which can change the beam energy by ±10 %, corresponding to a tuning range of ± 25 GHz.

Assuming the energy spread of the ion source to be 1 eV, one expects a residual Doppler width of about 5 MHz. To ensure full use of this basic resolution, the 60 kV acceleration voltage has to be controlled at the 10^{-5} level. Much effort

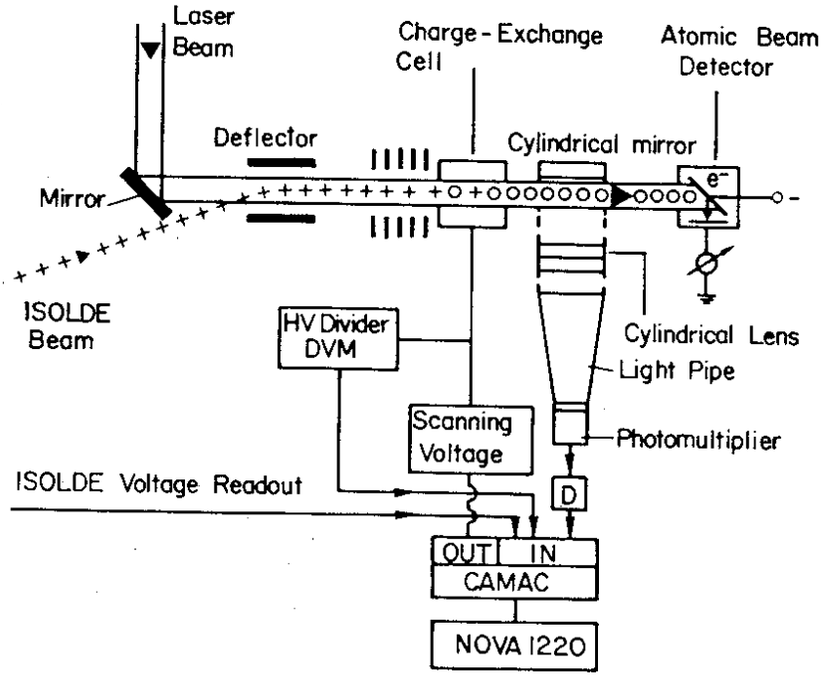

Figure 1
Schematic diagram of the experimental setup

was put into a stabilization system [6] which keeps the drift and ripple below this level, even at the high load from ionized air created by the pulsed proton beam. The main acceleration voltage, as well as the scanning voltage, is measured with an absolute accuracy better than 10^{-4}.

Figure 1 shows the essential parts of the apparatus in a schematic diagram. The ISOLDE beam is bent into the laser beam by means of an electrostatic deflector. It is accelerated or decelerated before entering the charge-exchange region. Resonance excitation of the neutralized beam is detected by observing the direct fluorescence. A cylindrical lens and a cylindrical mirror collect the photons which are focussed on the entrance slit of a light pipe and counted by means of a photomultiplier.

Isotope shift measurements require a direct comparison of resonance frequencies between different isotopes. A convenient reference is the line of the most abundant stable isotope, ^{138}Ba, which has a closed neutron shell, or one of the other stable isotopes with well-known IS relative to ^{138}Ba [5]. This comparison is made by alternately directing beams of different isotopes through the apparatus. At fixed laser frequency the shift between the resonances (in non-relativistic approximation)

$$\nu_2 - \nu_1 = \nu_0 \{ (2\,eU_1 / M_1c^2)^{\frac{1}{2}} - (2\,eU_2 / M_2c^2)^{\frac{1}{2}} \}$$

is given by the corresponding total acceleration voltages U_1 and U_2. The atomic masses M_1 and M_2 are taken from standard tables [7]. Their errors are usually of the order 10^{-6}.

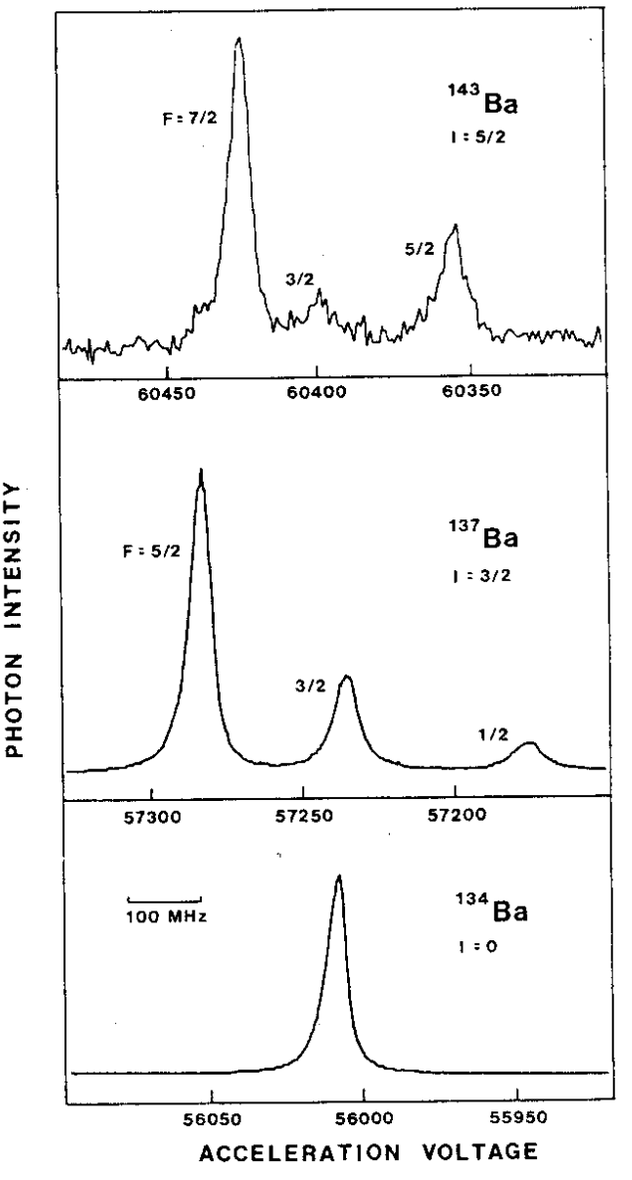

Figure 2
Example of a measurement for the case of ^{143}Ba (reference ^{137}Ba and ^{134}Ba)

RESULTS

Figure 2 shows the example of a measurement for ^{143}Ba. The rate of photomultiplier pulses is plotted versus the scanning voltage at the charge-exchange cell, added to the main acceleration voltage. The shift between the two stable reference isotopes, ^{137}Ba and ^{134}Ba, is used as a convenient on-line test of the high-voltage calibration. By transforming the voltage into the corresponding frequency scale one obtains a linewidth of about 30 MHz. The lines are thus somewhat Doppler-broadened due to the energy spread of the ion source and the beam divergence .

Similar measurements have been performed on $^{139-144}$Ba and ^{146}Ba, the beam intensity in the latter case being as low as 10^5 atoms per second. Each measurement has been repeated several times at different laser frequencies and, correspondingly, different voltages. The consistency of these measurements and the agreement with known results for the stable isotopes gives confidence in the basic accuracy of the voltage measuring equipment. The present analysis of the results is based on this accuracy limit which can be reduced by careful recalibration.

The isotope shifts $\delta\nu^{138,A} = \nu(A) - \nu(138)$, relative to ^{138}Ba, are compiled in Table 1. Corresponding differences of the mean-square nuclear charge radii $\delta\langle r^2\rangle$ have been calculated, following the procedure of Bekk et al. [5]. The errors of the latter are assumed to be 3%. They account for the unknown specific mass shift which is conventionally taken to be of the order of the normal mass shift.

Table 1
Isotope shifts $\delta\nu$ and deduced differences of mean-square charge radii $\delta\langle r^2\rangle$, relative to ^{138}Ba.

A	$\delta\nu^{138,A}$ (MHz)	$\delta\langle r^2\rangle^{138,A}$ (fm^2)
139	-473(6)	0.124(5)
140	-1075(6)	0.281(9)
141	-1505(8)	0.395(13)
142	-2019(7)	0.529(17)
143	-2493(11)	0.654(22)
144	-3027(10)	0.793(25)
146	-3893(15)	1.021(34)

Table 2 contains the hfs parameters a and b of the odd-A isotopes, from which the magnetic moments μ_I and spectroscopic quadrupole moments Q_S have been calculated.(see [5] and references therein). The spins are those predicted from nuclear spectroscopy. The intensities of the different hyperfine components within the spectra of ^{139}Ba, ^{141}Ba and ^{143}Ba confirm the spin values to be $I = 7/2$, $3/2$ and $5/2$, respectively.

Table 2
Nuclear spins I, hfs parameters a, b and deduced nuclear magnetic moments μ_I and spectroscopic quadrupole moments Q_S.

A	I	a (MHz)	b (MHz)	μ_I/μ_n	Q_S (b)
139	7/2	49(2)	-111(6)	-0.97(4)	-0.62(10)
141	3/2	41(3)	94(5)	-0.35(3)	0.52(9)
143	5/2	-32(4)	-178(8)	0.45(6)	-0.99(15)

DISCUSSION

The plot of $\delta\langle r^2\rangle$ for the barium series in Figure 3 shows the characteristic kink at the magic neutron number $N = 82$ which has already been observed in cesium [8, 9] and which follows the trend of $\delta\langle r^2\rangle$ in other isotones below and above $N = 82$ [10]. It can be explained in terms of nuclear deformation which enters into the mean-squared radius, and thus the IS, via the change of its mean-squared value $\delta\langle\beta^2\rangle$, according to [11]

$$\delta\langle r^2\rangle = (2/5)\,\rho\, R_0^2\, \delta A/A + (3/4\pi)\, R_0^2\, \delta\langle\beta^2\rangle$$

Here the first term represents the so-called standard isotope shift describing the expansion of a uniformly charged liquid drop of radius R_0. It is multiplied by an empirical factor $\rho = 0.5$ which fits the overall trend of isotope shifts and which has some theoretical support in the droplet model [12]. For comparison, this reduced standard shift is represented in Figure 3 by the slope of lines corresponding to different rms deformation parameters $\langle\beta^2\rangle^{1/2}$. The reference value for ^{138}Ba: $\langle\beta^2\rangle^{1/2} = 0.092(2)$ is taken from the B(E2) value [13].

The magnetic moments and spectroscopic quadrupole moments of the odd-A isotopes are well reproduced by particle-rotor calculations based on the Nilsson model [14]. In particular, the apparent anomalous behaviour in the sequence of spectroscopic

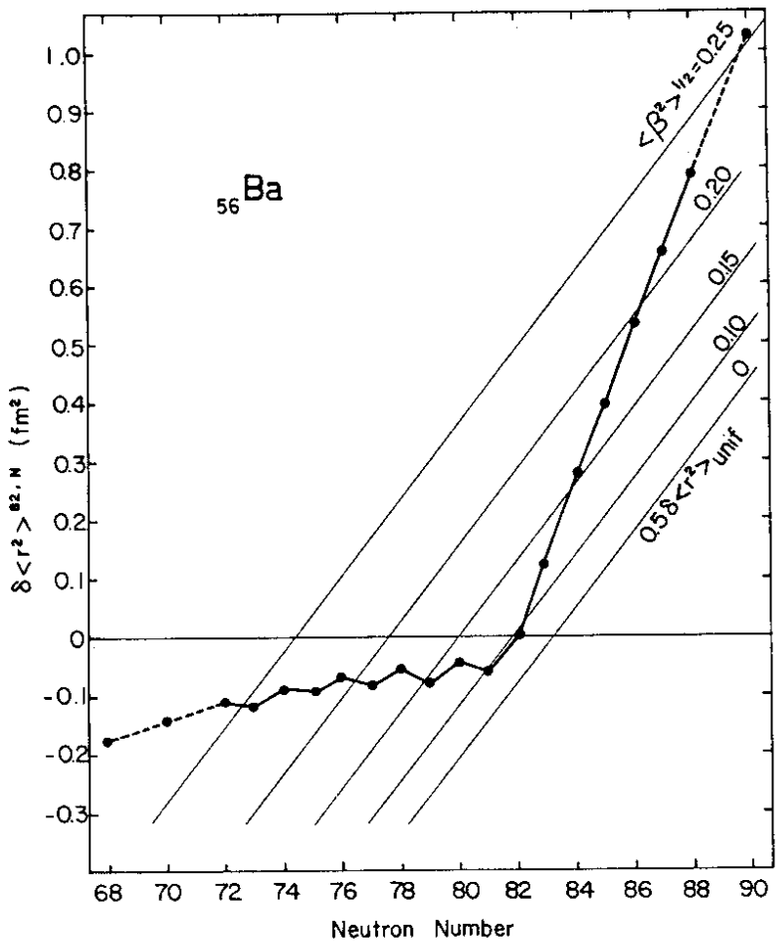

Figure 3
Plot of $\delta\langle r^2\rangle$ for the series of barium isotopes. N>82: this work, N<82: Bekk et al. |5|. The assumption $\rho = 0.5$ is made for lines of constant $\langle\beta^2\rangle^{1/2}$.

quadrupole moments is explained by the main components of the nuclear wave functions being due to the low-Ω Nilsson levels originating from the $f_{7/2}$ and $h_{9/2}$ shell-model states. The deformation parameters obtained from the nuclear moments are slightly larger than those evaluated from the isotope shifts. The general trend of deformation, gradually increasing with mass number, is, however, well reproduced.

FINAL REMARK

This work will be continued to complete the presently available data on neutron-deficient barium isotopes |5|. Since the information on cesium is rather complete |9|, it will be most attractive to look at the isotonic changes of nuclear "gross" properties, such as radii and deformation, in more detail. In fact, collinear-beam laser spectroscopy appears to be a versatile instrument for further systematic studies in that direction. It can be applied either to the neutralized atomic beams or directly to the ion beams of on-line isotope separators. Silverans et al. |15| demonstrated this latter variant of the method with a beam of radioactive ^{140}Ba ions. On the other hand, charge-exchange neutralization seems to open up a quite general way to the spectra of neutral atoms which are more easily accessible to dye lasers. This was again confirmed in a recent successful attempt on some neutron-deficient ytterbium isotopes.

This work was sponsored by the Deutsche Forschungsgemeinschaft and the Bundesministerium für Forschung und Technologie.

REFERENCES

|1| Anton, K.-R., Kaufman, S.L., Klempt, W., Moruzzi, G., Neugart, R., Otten, E.W. and Schinzler, B., Hyperfine Interactions 4 (1978) 87-90 and Phys. Rev. Lett. 40 (1978) 642-645.

|2| Schinzler, B., Klempt, W., Kaufman, S.L., Lochmann, H., Moruzzi, G., Neugart, R., Otten, E.W., Bonn, J., Reisky, L.v., Spath, K.P.C., Steinacher, J. and Weskott, D., Phys. Lett. 79B (1978) 209-212. Klempt, W., Bonn, J. and Neugart, R., Phys. Lett. 82B (1979) 47-50.

|3| Carraz, L.C., Sundell, S., Ravn, H.L., Skarestad, M. and Westgaard, L., Nucl. Instr. and Meth. 158 (1979) 69-80.

|4| Kaufman, S.L., Opt. Commun. 17 (1976) 309-312.

|5| Bekk, K., Andl, A., Göring, S., Hanser, A., Nowicki, G., Rebel, H. and Schatz, G., Z. Physik A291 (1979) 219-230.

|6| Georgi, K.-H. and Vosicki, B., to be published.

|7| Wapstra, A.H. and Bos, K., Atomic Data and Nuclear Data Tables 19 (1977) 177-214.

|8| Bonn, J., Klempt, W., Neugart, R., Otten, E.W. and Schinzler, B., Z. Physik A289 (1979) 227-228.

|9| Huber, G., Touchard, F., Büttgenbach, S., Thibault, C., Klapisch, R., Liberman, S., Pinard, J., Duong, H.T., Juncar, P., Vialle, J.L., Jacquinot, P. and Pesnelle, A., Phys. Rev. Lett. 41 (1978) 459-462. Thibault, C., Contribution to this conference.

|10| Heilig, K. and Steudel, A., Atomic Data and Nuclear Data Tables 14 (1974) 613-638.

|11| Ullrich, S. and Otten, E.W., Nucl. Phys. A248 (1975) 173-190.

|12| Myers, W.D., Phys. Lett. 30B (1969) 451-454.

|13| Christy, A. and Häusser, O., Nucl. Data Tables 11 (1972) 281-298.

|14| Larsson, S.E., Leander, G. and Ragnarsson, I., Nucl. Phys. A307 (1978) 189-223.

|15| Silverans, R.E., Borghs, G. and Van den Cruyce, J.-M., Contribution to this conference.

6